# Estimation of states under Colored Measurement Noise (CMN) using UFIR and Kalman Filters modified

[1]ELI G. PALE-RAMON, [1]YURIY S. SHMALIY, [2]LUIS J. MORALES-MENDOZA,
[2]MARIO GONZÁLEZ-LEE, [2]SILVERIO PÉREZ-CACERES,
[2]EFRÉN MORALES-MENDOZA

[1]Electrical Engineering Department, Universidad de Guanajuato, Salamanca,
Guanajuato, 36680, MEXICO
[2]Electronics Engineering Department, Universidad Veracruzana,
Poza Rica, Veracruz, 93380, MEXICO

*Abstract:* The estimate process of a moving target trajectory is a well-known problem, where the main objective is to improve the estimation of object position. During the tracking are presented errors or variations between the true position and the estimated. In this paper, we treat such variations as a Gauss-Markov colored measurement noise (CMN). The estimation process is performed in predict and update, where the prediction indicates the next position of the bounding box, and the update is a correction step, which includes the new measurement of the tracking model and helps to improve the estimation. Looking for this improvement we use Kalman and Unbiased Finite Impulse Response filters in the standard version and modified for CMN to demonstrate the filter with the best performance. To test the most robust filter we use a high coloredness factor. The tests were carried out with simulated data (ideal and no ideal conditions) and with benchmark data (no ideal conditions). The UFIR modified for the CMN algorithm showed favorable results with high precision and low RMSE in the object tracking process with benchmark data and under no ideal conditions. While KF CMN showed better results under ideal conditions.

*Key-Words:* Bounding box, colored measurement noise, estimation, Kalman filter, precision, tracking, Unbiased FIR filter

Received: June 7, 2021. Revised: September 5, 2022. Accepted: September 28, 2022. Published: October 25, 2022.

## 1 Introduction

The object tracking process is a widely researched topic and has a wide range of applications in the fields of visual navigation, robotics, intelligent transportation, and security, among others [1, 2]. There are different research approaches, however, it continues to present challenges in their treatment, there is no single approach capable of overcoming all the impact factors that affect the tracking algorithm's performance.

Object tracking can be defined as the problem of estimating the trajectory of an object as it moves around a scene [3, 4]. This process is usually accompanied by variations in position, that is, the target is not tracked exactly. There are variations in the estimate, that is, there is a discrepancy between the real position and the estimated position. These variations can be considered as colored measurement noise (CMN) that is not white [5].

The variations in object tracking can be more clearly identified, during the tracking process, if we use a bounding box to contain the information of the object to be tracked. The bounding boxes generated by the tracking algorithm do not always detect the target object, they may detect another object in the scene, or they do not detect the exact shape of the target. This may be due to various factors affecting the tracking process, such as camera movement, occlusion, or blurred scene, among others. In this sense, a method that has proven to be effective in avoiding large errors in the tracking process is the use of a motion model and state estimators. [5–9]. If the state-space model is correct, it can very accurately represent the trajectory of the tracked object. However, the performance of the tracking algorithm will still depend on measurement and process noise.

For these reasons, in this paper, we use Kalman (KF) and Unbiased Finite Impulse Response (UFIR) in their versions standard and modified to minimize the error in the estimation, seeking to stabilize the trajectory and size of the bounding box to obtain an algorithm that produces greater precision in tracking tasks. The process of state estimations were performed in two phases of recursions and iterations: ”predict” and ”update”. Using root mean square errors and the precision to measure the performance of the algorithms.

## 2 Object processing

In order to carry out the object-tracking process, it is necessary to identify the object to track. The image processing operations look for the best recognition of the objects tracked. Therefore, it is necessary to identify the appropriate characteristics to differentiate the target from other objects and the background scene. The content of an object can be described through its properties. There are different ways to locate a target, for example, its contour or finding the pixels of

the object, one of the most used shape parameters in object tracking is the bounding box, [10].

### 2.1 Bounding box

The bounding box (BB) is a rectangular box that encloses all the objects in a scene and can be used to represent an object during tracking. Using the BB as a shape parameter in the tracking process, the information about the position of the objects is contained in an array of bounding boxes. The BB matrix consists of 4 columns and n rows, the number of rows corresponds to the total number of detections, while the columns represent the dimensions of the bounding boxes: coordinate "x", coordinate "y", width (xw), height (yw) [11].

The information about the "x", "y" coordinates, the height and the width of the BB, is used to estimate the position of the object during the tracking process. However, there may be errors in the position estimation. In this sense, the use of a filtering method is an effective method, its aim is to mitigate the noise present in tracking process. A filtering method is used to predict the coordinates of BB. The estimation method consists of 2 steps: prediction and correction. The prediction indicates the next position of the bounding box based on its previous position. The update is a correction step, which includes the new measurement of the tracking model and helps to improve the estimate of the filtering [12, 13].

## 3 State-space model of tracking object

We consider a moving object with observation corrupted by CMN can be represented in discrete-time state-space with the following state and observation equations:

$$\begin{aligned} x_n &= A_n x_{n-1} + B_n w_n \,, && (1)\\ v_n &= \Psi_n v_{n-1} + \xi_n \,, && (2)\\ y_n &= C_n x_n + v_n \,, && (3) \end{aligned}$$

where $x_n \in \mathbb{R}^K$ is the state vector, $y_n \in \mathbb{R}^M$ is the observation vector, $v_n \in \mathbb{R}^M$ is the colored Gauss-Markov noise, and $A_n \in \mathbb{R}^{K\times K}$ is the state transition matrix, $B_n \in \mathbb{R}^{K\times P}$ is the gain matrix model, $C_n \in \mathbb{R}^{M\times K}$ is the measurement matrix. Measurement noise transfer matrix $\Psi_n$ is chosen such that the colored noise $v_n$ remains stationary. The zero mean Gaussian noise vectors $w_n \sim \mathcal{N}(0, Q_n) \in \mathbb{R}^P$ and $\xi_n \sim \mathcal{N}(0, R_n) \in \mathbb{R}^M$ have the covariances $Q_n$ and $R_n$ and the property $E\{w_n \xi_k^T\} = 0$ for all $n$ and $k$. We will consider the following estimates: the prior estimate $\hat{x}_n^- \triangleq \hat{x}_{n|n-1}$, posterior estimate $\hat{x}_n \triangleq \hat{x}_{n|n}$, prior estimation error $\epsilon_n^- = x_n - \hat{x}_n^-$, the posterior estimation error $\epsilon_n = x_n - \hat{x}_n$, the prior error covariance $P_n^- \triangleq P_{n|n-1} = E\{\epsilon_n^- \epsilon_n^{-T}\}$, and the posterior error covariance $P_n \triangleq P_{n|n} = E\{\epsilon_n {\epsilon_n}^T\}$.

The matrices for the model were built considering a constant velocity model [14]. For the moving object state space model, the state transition A is a block diagonal matrix with:

$$\begin{bmatrix} 1 & \tau \\ 0 & 1 \end{bmatrix}, \qquad (4)$$

where $\tau$ is the sample time. This block is repeated for the 4 coordinates of the bounding box.

The matrix B is given by equation (5), this set of 3 by 1 is repeated for each coordinate of bounding box corners. Finally, it will obtain a matrix with dimensions 12 by 4 , in which the equation (5) forms a diagonal.

$$B = \begin{bmatrix} \frac{\tau^2}{2} \\ \tau \end{bmatrix}, \qquad (5)$$

The observation matrix (C) is defined as shown below:

$$C = \begin{bmatrix} 1 & 0 & 0 & 0 & 0 & 0 & 0 & 0 \\ 0 & 0 & 1 & 0 & 0 & 0 & 0 & 0 \\ 0 & 0 & 0 & 0 & 1 & 0 & 0 & 0 \\ 0 & 0 & 0 & 0 & 0 & 0 & 1 & 0 \end{bmatrix}. \qquad (6)$$

### 3.1 Avoid the CMN

To avoid the CMN $v_n$ in $y_n$ is necessary the model modification using measurement differencing. For which, it is considered a new observation $z_n$ as a measurement difference.

$$\begin{aligned} z_n &= y_n - \Psi_n y_{n-1} \,, \\ &= C_n x_n + v_n - \Psi_n H_{n-1} x_{n-1} - \Psi_n v_{n-1} \qquad (7) \end{aligned}$$

and transform (7) to

$$z_n = D_n x_n + \bar{v}_n \,, \qquad (8)$$

where $D_n = H_n - \Gamma_n$, $\Gamma_n = \Psi_n H_{n-1} F_n^{-1}$, $\bar{v}_n = \Gamma_n B_n w_n + \xi_n$, noise $\bar{v}_n$ is now white with the properties

$$\begin{aligned} \bar{R}_n = E\{\bar{v}_n \bar{v}_n^T\} &= \Gamma_n \Phi_n + R_n \,, && (9)\\ E\{\bar{v}_n w_n^T\} &= \Gamma_n B_n Q_n \,, && (10) \end{aligned}$$

where $\Phi_n = B_n Q_n B_n^T \Gamma_n^T$, and model (1) and (2) has thus two white and time-correlated noise sources $w_n$ and $\bar{v}_n$.

## 4 Kalman Filter modified for CMN

In estimating the system state through the coordinates of the BB, we can use the Kalman filter(KF). Within

which the state is assumed to be distributed by white Gaussian noise with mean zero. The estimate process consists of two steps, prediction, and update. In this case, the KF is recursive [15], which means that the previously estimated state must be combined with new observation to calculate the best estimate of the current state. One of the important aspects to consider when using the KF algorithm is that it requires knowledge of the system parameters, initial values, and measurement noise.

The KF can estimate the state dynamics of the system iteratively [16]. Assuming that the process noise $w_n$ is white Gaussian with zero mean, the prior state estimate is computed by (11).

$$\hat{x}_n^- = A\hat{x}_{n-1} + B_n w_n \tag{11}$$

Next, in the update step, the current prior predictions are combined with the current state observation to redefine the state estimate and the error covariance matrix. To obtain the optimal state estimate is combined the prediction with the current observation, and now it is called the posterior state estimate. The measurement $z_n$ is corrupted by a factor of colored measurement noise $\Psi_n$(12).

$$z_n = y_n - \Psi_n y_{n-1} \tag{12}$$

The residual covariance matrix is obtained as follow:

$$S_n = C_n P_n^- C_n^T + R_n \tag{13}$$

The measurement residual is

$$\begin{aligned} s_n &= z_n - D_n\hat{x}_n^- \\ &= D_n A_n \epsilon_{n-1} + D_n B_n w_n + \bar{v}_n\,, \end{aligned} \tag{14}$$

the innovation covariance $S_n$ is given by

$$\begin{aligned} S_n &= E\{s_n s_n^T\} \\ &= D_n P_n^- D_n^T + R_n + C_n\Phi_n + \Phi_n^T D_n^T \end{aligned} \tag{15}$$

and the estimation of KF for CMN is

$$\begin{aligned} \hat{x}_n &= \hat{x}_n^- + K_n s_n \\ &= A_n\hat{x}_{n-1} + K_n(z_n - D_n A_n \hat{x}_{n-1})\,, \end{aligned} \tag{16}$$

where $K_n$ is the bias correction gain that should be optimized for correlated $w_n$ and $\bar{v}_n$. the estimation error $\epsilon_n$ can be written as

$$\begin{aligned} \epsilon_n &= x_n - \hat{x}_n \\ &= (I - K_n D_n)A_n\epsilon_{n-1} \\ &\quad +(I - K_n D_n)B_n w_n - K_n\bar{v}_n \end{aligned} \tag{17}$$

and the error covariance $P_n = E\{\epsilon_n\epsilon_n^T\}$ transformed to

$$\begin{aligned} P_n &= P_n^- - (P_n^- D_n^T + \Phi_n)K_n^T - K_n(P_n^- D_n^T + \Phi_n)^T \\ &\quad +K_n S_n K_n^T\,, \end{aligned} \tag{18}$$

where $P_n^-$ is given by (18) and $S_n$ by (14). The optimal gain $K_n$ is given by

$$K_n = (P_n^- D_n^T + \Phi_n)S_n^{-1} \tag{19}$$

and (18) becomes

$$P_n = P_n^- - K_n(D_n P_n^- + \Phi_n^T)\,. \tag{20}$$

A pseudo-code of the KF algorithm for CMN with correlated $w_n$ and $\bar{v}_n$ is listed as Algorithm 1. It can be observed, if the value $\Psi_n = 0$, the algorithm becomes the standard Kalman filter algorithm.

**Algorithm 1:** KF for CMN and Correlated $w_n$ and $\bar{v}_n$

**Data:** $\mathbf{y}_n$, $\hat{x}_0$, $\mathbf{P}_0$, $\mathbf{Q}_n$, $\mathbf{R}_n$
**Result:** $\hat{\mathbf{x}}_n$, $P_n$

**begin**
  **for** $n = 1, 2, \cdots$ **do**
    $D_n = H_n - \Psi_n C_{n-1} A_n^{-1}$
    $z_n = y_n - \Psi_n y_{n-1}$
    $P_n^- = A_n P_{n-1} A_n^T + B_n Q_n B_n^T$
    $S_n = D_n P_n^- D_n^T + R_n + C_n\Phi_n + \Phi_n^T D_n^T$
    $K_n = (P_n^- D_n^T + \Phi_n)S_n^{-1}$
    $\hat{x}_n^- = A_n\hat{x}_{n-1}$
    $\hat{x}_n = \hat{x}_n^- + K_n(z_n - D_n\hat{x}_n^-)$
    $P_n = (I - K_n D_n)P_n^- - K_n\Phi_n^T$
  **end for**
**end**

# 5 Unbiased Finite Impulse Response Filter modified for CMN

In the same way as the KF, the UFIR filter can also be generalized to colored measurement noise, considering that the unbiased average ignores zero average noise. Next, we work with a modification to the UFIR filter for CMN.

As already mentioned, the KF requires noise information. In the case of the UFIR filter, this requirement is not necessary, except for the assumption of a zero mean [2, 4, 9, 17, 18]. For this reason, it is considered to be more suitable for use in object tracking as databases with incomplete information or in time tracking, in which information about measurement and process noises is not always known exactly. In the UFIR filter, $w_k$, and $\hat{v}_n$ can be ignored and therefore the UFIR is unique for correlated and no-correlated $w_k$, and $\hat{v}_n$. So its equation of state is given by $x_n = F_n x_{n-1}$.

The state estimation is done in two steps. In the prediction step, only the state (5) is calculated a priori, because the UFIR filter does not require knowing the statistical noise information. However, UFIR

requires an optimal averaging horizon [m, n] to minimize the mean square error (MSE), that is, it operates simultaneously with N measurements on a horizon $[m,k]$ of $m=k-N+1$. The UFIR filter cannot ignore the CMN $v_n$, which violates the zero-mean assumption at short horizons [19,20].

Since we use an iterative algorithm using recursion, in the update step, the state estimate is combined with the actual observation state to refine the state. The estimate is iteratively updated in a posteriori state using: Matrix G, measurement residuals, and the bias correction Gain.

A Matrix G or better known as generalized noise power gain (GNPG) (21), the measurement residual, and the bias correction gain.

$$G_l=[D_l^TD_l+(F_nG_{l-1}F_l^T)^{-1}]^{-1} \tag{21}$$

The measurement residual $z_l$ is given by:

$$z_l=y_l-\Psi_l y_{l-1} \tag{22}$$

In the UFIR filter, the estimation errors are taken into acount only on the horizon $[m,k]$ and it is computed in term of GNPG. The bias correction gain can be expressed as:

$$K_l=G_lD_l^T \tag{23}$$

Then, it is computed the a posteriori state estimate as follow:

$$\bar{x}_l=\bar{x}_l^-+K_l(z_l-D_l\bar{x}_l^-); \tag{24}$$

Since the CMN is present in the tracking process data, The recursive computation of the posterior estimate to avoid the CMN can be summarized in the following pseudo-code, as shown in Algorithm 2. To initialize the iterations, the algorithm requires a short measurement vector $y_(m.k)=[y_m\ldots y_k]^T$ and a matrix (25).

$$H_{m,s}=\begin{bmatrix} D_m(F_s\ldots F_{m+1})^{-1} \\ \vdots \\ D_{s-1}F_s^{-1} \\ D_s \end{bmatrix}. \tag{25}$$

Note that $C_{m,s}^TC_{m,s}$ is singular if $s-m<K-1$, and thus the generalized noise power gain $G_s$ cannot be calculated on horizons shorter than K points. In the same way as with the KF filter modified for CMN, when the coloredness factor $\Psi_n=0$, the Algorithm 2, UFIR modified for CMN, becomes the standard UFIR filter [19,20].

Since UFIR filter operates on the horizon $[m,k]$ of the total horizon N. To minimize MSE, the horizon to work with must be optimized as $N_{opt}$. According to [5] we can determine $N_{opt}$, by the following equation:

$$N_opt=\frac{12\sigma_\xi}{\tau^2\sigma_w} \tag{26}$$

**Algorithm 2:** UFIR Filter for CMN

**Data:** $N$, $y_n$
**Result:** $\hat{x}_n$
**begin**
  **for** $n=N-1,N,\cdots$ **do**
    $m=n-N+1$ , $s=n-N+K$
    $G_s=(C_{m,s}^TC_{m,s})^{-1}$
    $\bar{x}_s=G_sC_{m,s}^TY_{m,s}$
    **for** $l=s+1:n$ **do**
      $D_l=H_l-\Psi_lH_{l-1}F_l^{-1}$
      $z_l=y_l-\Psi_ly_{l-1}$
      $G_l=[D_l^TD_l+(F_lG_{l-1}F_l^T)^{-1}]^{-1}$
      $K_l=G_lD_l^T$
      $\bar{x}_l^-=F_l\bar{x}_{l-1}$
      $\bar{x}_l=\bar{x}_l^-+K_l(z_l-D_l\bar{x}_l^-)$
    **end for**
    $\hat{x}_n=\bar{x}_n$
  **end for**
**end**

Another method to calculate the optimal horizon $N_{opt}$ is using measurement residuals, given the property that the derivative of its trace with respect to the length of the horizon reaches a minimum when N tends to $N_{opt}$. This allows determining Nopt, through the minim value of MSE. This is a useful property when ground truth is not available. [5,20].

# 6 Performance metrics of tracking algorithm

A widely used statistical metric to evaluate the tracking algorithm performance, from an overall perspective, is the root mean square error (RMSE). But, the most common metric used to evaluate tracking performance is precision.

## 6.1 Precision

Performance evaluation of tracking algorithms can be evaluated by precision metric. Precision can be defined as the percentage of the number of correct predictions over the total number of predictions. [21,22].

Before establishing the precision calculation, it is necessary to obtain another metric, intersection over union (IoU). The IoU can be defined as the percentage overlap of the predicted bounding box over the true bounding box (TBB). The equation for the calculation of IoU is shown below:

$$IoU=\frac{IA}{(TBB-EBB)-IA} \tag{27}$$

Where the IA is the area of intersection between the bounding box of the target object, the true bounding

box (TBB), and the estimated bounding box (EBB). The TP is a true positive, and FP is a false positive.

As already mentioned, the precision is calculated from the IoU value for which it is necessary to establish an evaluation parameter, for this, an IoU threshold is established [21, 23]. The equation for calculating precision is:

$$Precision = \frac{\Sigma TP}{\Sigma TP + \Sigma FP} \tag{28}$$

Where TP is True Positive, that is a correct detection of a bounding box, that is, the IoU between the EBB and TBB is greater than or equal to the established threshold value. FP is False positive, which is an incorrect detection of an object or an off-site detection. The IoU is less than the given threshold value but greater than zero. FN is a false negative.

# 7 Object tracking test results

## 7.1 Results of simulation test

The simulation was performed using the object tracking model can be described by (1) and (2) and the known matrices. For the first simulation test, we considered that a target is disturbed by white Gaussian acceleration noise with a standard deviation of $\sigma_w = 2m/s^2$. The data noise originates from white Gaussian with $\sigma_\xi = 30$ m. The trajectory simulation was 2000 points with sample time $T = 0.05$ seconds, $P_0 = 0$, $Q = \sigma_w^2$, $R = \sigma_V^2$, on a short horizon $N_opt = 60$.

The RMSE obtained by the standard and modified filters for CMN, KF and UFIR, from the coloredness factor $\Psi$ 0 to 0.95 are shown in Fig. 1 a). The Nopt for UFIR has used the same size for the entire range of $\Psi$. Standard UFIR results are shown with a magenta line, standard KF with a black line, and UFIR CMN with a red line. For the KF CMN, the object tracking model were established under ideal conditions, $p = q = 1$, and with no ideal conditions, $p \neq 1$, represented with blue line, and $q \neq 1$ with blue dotted line.

Assuming that noise information is incomplete, in Fig. 1 a) are shown the relevant filtering errors produced by substituting $Q$ with $p^2Q$ and $R$ with $q^2R$ for $\{p, q\} > 0$ [5, 19]. As can be seen, even slight modifications in error factors ($p = 2, q = 0.5$) make the KF CMN less accurate than the UFIR CMN. It even has poorer performance than standard filters. The UFIR and KF algorithms produced a high values of RMSE with similar behavior on the all coloredness factor $\Psi$ range. Therefore, we consider that tmodified filters foe CMN showed better results with lower. under ideal conditions the performance of KF CMN is slightly lower than UFIR CMN, remembering that this depends largely on the correct dynamic model.

To corroborate the effect of incomplete noise information. We performed another test considering the relevant filtering errors produced by substituting in the algorithms $Q$ with $p^2Q$ and $R$ with $q^2R$ for $\{p, q\} > 0$, ($p = 2, q = 0.5$), and ($p = 0.5, q = 2$) The results obtained are shown in Fig. 1 b).

As can be seen, a slight modification of the error factor generates a significant change in the performance of the KF CMN, with which a worse performance was obtained than that obtained under ideal conditions. With this we can corroborate that the performance of the KC CMN is highly related to the correct establishment of the state model. On the other hand, UFIR is more robust when the noise information is not available. Also, the UFIR filter does not require knowing the noise conditions $Q$ and $R$ it shows that the UFIR CMN is preferable for object tracking. This gives another proof that the UFIR CMN is more suitable for object tracking in real case or with benchmark data without complete noise information.

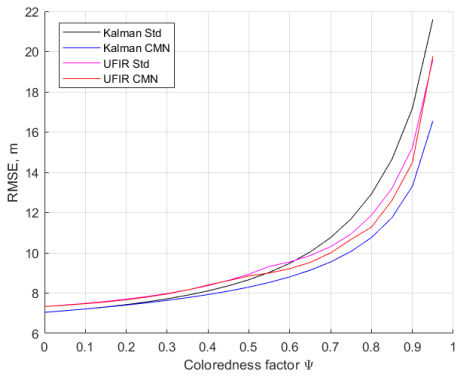


(a) KF and UFIR standard and modified filters

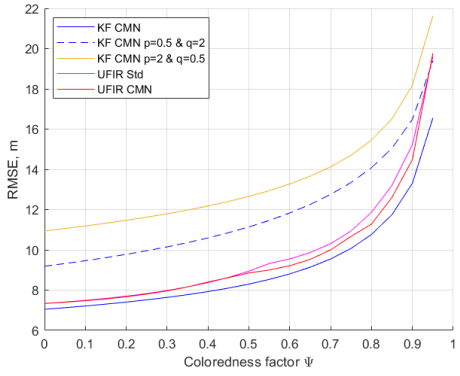


(b) KF and UFIR modified for CMN with the incomplete information

Figure 1: RMSE results obtained by the KF and UFIR standard and modified filters

### 7.2 Results of benchmark data test

In this section, we used for test benchmark data [24]. The data is called "SUV". Taking into account the tests carried out in the previous subsection, the test was performed with the highest coloredness factor $\Psi = 0.95$ in order to evaluate the robustness of the algorithms.

The object tracking model considered that the car target is disturbed by white Gaussian acceleration noise with the standard deviation of $\sigma_w = 3m/s^2$. The data noise (CMN) originates from white Gaussian $\sigma_v = 2m$. The trajectory is measured each sample time T= 0.05 seconds, $P_0 = 0$, $Q = \sigma_w^2$, $R = \sigma_V^2$, on a short horizon $N_opt = 60$. The model of a moving object is completed according to the section 3.

Then, to compare the performances of the UFIR and Kalman filters consider the moving vehicle tracking problem, we examine the results of the benchmark SUV test, where we used the bounding box coordinates as a tool for metric evaluation. In Fig.2 to plot the true estimated object trajectory, we use the bounding box centroids, where the gray line is the ground truth, the black line is KF standard (KF std), the blue line is KF modified for CMN (KF CMN), the magenta line is UFIR standard (UFIR Std) and the red line is UFIR modified for CMN (UFIR CMN). The graphed trajectories correspond to the coordinates on the "x" and "y" axis of the centroid of each one of the bounding boxes of the tracking of the moving object. The trajectory followed by the object does not correspond to a straight line; we can observe curved paths. The standard algorithms UFIR and KF present greater differences concerning the true trajectory; while UFIR CMN and KF CMN presented a closer estimate. Given the type of trajectory made by the object, visual analysis is difficult, the difference between the estimates is especially neatly with the root mean square error results. The RMSE values were 51.00 for UFIR CMN, 55.67 for KF CMN, 57.97 for UFIR std, and 79.97 for KF std. Over the entire trajectory, the standard filters generates larger errors than the filter modified for CMN. According to these results, we consider that the algorithms modified for CMN presented a good performance with a high value of $\psi$. While, the KF std showed a poor performance.

To have a better perspective of the performance of the algorithms, Fig.3 shows the bounding boxes of a random point in the trajectory, in which it can be seen that UFIR CMN presents a closer estimate, followed by KF CMN, while KF std shows poor performance on position and size compared to the ground truth bounding box. One of the improvements expected by the algorithms used is the stabilization of the bounding boxes both in their trajectory and in their size. From these results, we can see that UFIR CMN

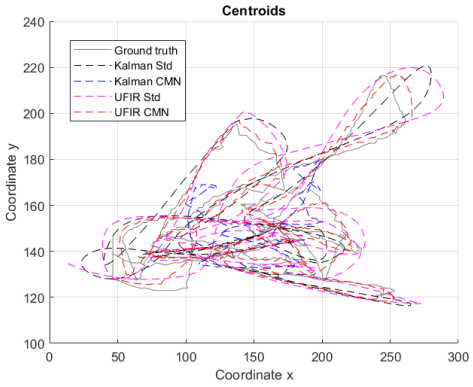


Figure 2: Centroids estimation in the x-y plane ($Nopt = 60$),with $\Psi = 0.95$.

and KF CMN provide an improvement in object estimation. To determine the algorithm that presented the best performance, the precision metric is used as shown below.

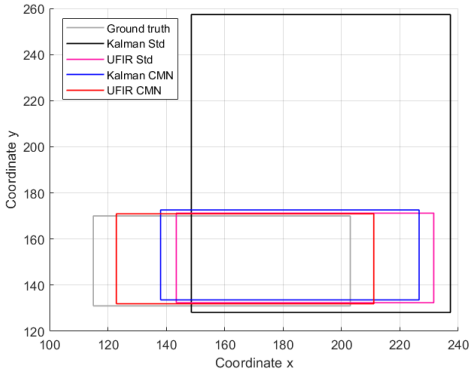


Figure 3: Bounding box estimation.

The filter precision in the entire intersection over the union (IoU) threshold range is shown in Fig.4. The UFIR CMN and KF CMN filters presented the best precision with a similar behavior up to the threshold of 0.2, this means that the precision is close to 1 when the Predicted Bounding Box (PBB) overlaps at least over 20% of true Bounding Box (TBB). At this threshold level, it can be inferred that in each algorithm both standard and modified for CMN present good results, however the most used thresholds as a parameter to measure the performance of the algorithms are 0.5 and 0.75 [21], being 0.5 the most conventional. Taking as reference the threshold of 0.5, which can be inferred that the PBB overlaps at least the 50% of the TBB. With these results, we can determine that the UFIR CMN filter has a higher precision than KF CMN, with a significant difference. If we take into account a threshold of 0.75, we again find that UFIR CMN presents the best performance with

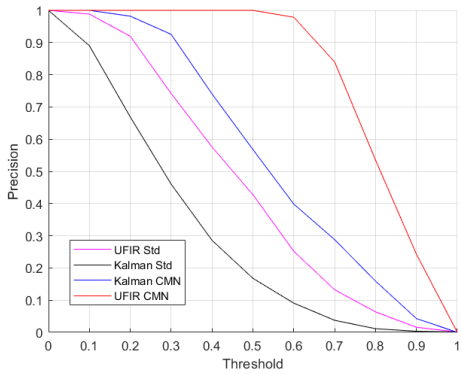


Figure 4: Precision of benchmark "SUV"($Nopt = 60$),with $\Psi = 0.95$.

a precision close to $0.7$, while the precision for KF CMN is around $0.3$. UFIR CMN performs best until the $0.8$ threshold, although its precision value at this point is around $0.5$. Therefore, we consider that the UFIR CMN algorithm provided better results in a wide threshold range, followed by KF CMN, which we consider had an acceptable performance up to the threshold of $0.5$, which corresponds to the most used threshold IoU range for evaluate the performance of algorithms. On the other hand, the UFIR and KF filters in their standard version showed poor performance, since at the threshold of $0.5$ the precision of the standard UFIR is less than $0.5$ and the precision of the standard KF is close to $0.3$. Since, the precision focuses on the percentage of the true bounding box detected. From this test, it can be determined that under a high coloredness factor $\Psi = 0.95$ the UFIR CMN filter obtained the best performance.

## 8 Conclusions

It was shown that the modified KF and UFIR algorithms derived from the differentiation of measurements for the colored measurement noise are better than the standard KF and UFIR filters, both analytically and numerically, for the estimation of states in the object tracking process.

The examples of simulations of the tracking problem confirm the theoretical inferences that under ideal conditions, with complete noise information, the KF CMN filter presents a better performance with lower typical RMSE values.

According to the second experiment with data simulation under non-ideal conditions, it is verified that the UFIR CMN works better in scenarios where the information is not complete and is more robust to an inadequate establishment of the dynamic model. because the UFIR filter does not require knowing the statistical noise information.

In addition, with the experimental example of visual object tracking based on the benchmark "SUV" in presence of CMN with the highest coloredness factor. It is shown that the modified KF and UFIR algorithms adjusted correctly have the ability to suppress CMN efficiently and provide state estimation with higher precision than standard filters.

Based on the results of this work, we found that the UFIR modified for CMN presented a better performance, since it provides an estimation of the state with greater precision and lower estimation error based on RMSE. It is proving to be more robust under scenarios of incomplete or unknown noise information and with the highest coloredness factor. These characteristics make it a highly applicable algorithm in cases with tracking models where the information is not well known or complete information is not available.

Therefore, we conclude that the use of modified UFIR for CMN would contribute to the development of applications and research and the improvement of tracking tasks. We are currently working on modifications to the UFIR CMN algorithm, focused on improving estimates when the values of $\Psi$ and IoU threshold are the highest.

*References:*

[1] A. Yilmaz, O. Javed, and M. Shah, "Object tracking: A survey," *Acm computing surveys (CSUR)*, vol. 38, no. 4, pp. 13–es, 2006.

[2] T. Kang, Y. Mo, D. Pae, C. Ahn, and M. Lim, "Robust visual tracking framework in the presence of blurring by arbitrating appearance-and feature-based detection," *Measurement*, vol. 95, pp. 50–69, 2017.

[3] M. Parmar, "A survey of video object tracking methods," _, p. 40, 2016.

[4] H. S. Parekh, D. G. Thakore, and U. K. Jaliya, "A survey on object detection and tracking methods," *International Journal of Innovative Research in Computer and Communication Engineering*, vol. 2, no. 2, pp. 2970–2978, 2014.

[5] Y. S. Shmaliy, S. Zhao, and C. K. Ahn, "Kalman and ufir state estimation with coloured measurement noise using backward euler method," *IET Signal Processing*, vol. 14, no. 2, pp. 64–71, 2020.

[6] D. Simon, *Optimal state estimation: Kalman, $H_\infty$, and nonlinear approaches*. Hoboken,NJ: John Wiley & Sons, 2006.

[7] P. Liang, E. Blasch, and H. Ling, "Encoding color information for visual tracking: Algorithms and benchmark," *IEEE transactions on*

*image processing*, vol. 24, no. 12, pp. 5630–5644, 2015.

[8] Y. S. Shmaliy, "Linear optimal fir estimation of discrete time-invariant state-space models," *IEEE Transactions on Signal Processing*, vol. 58, no. 6, pp. 3086–3096, 2010.

[9] S. Zhao, Y. S. Shmaliy, and F. Liu, "Fast computation of discrete optimal fir estimates in white gaussian noise," *IEEE Signal Processing Letters*, vol. 22, no. 6, pp. 718–722, 2014.

[10] W. Burger, M. J. Burge, M. J. Burge, and M. J. Burge, *Principles of digital image processing*. Springer, 2009, vol. 54.

[11] K. Choeychuen, P. Kumhom, and K. Chamnongthai, "An efficient implementation of the nearest neighbor based visual objects tracking," in *2006 International Symposium on Intelligent Signal Processing and Communications*. IEEE, 2006, pp. 574–577.

[12] P. Deepak and S. Suresh, "Design and utilization of bounding box in human detection and activity identification," in *Emerging ICT for Bridging the Future-Proceedings of the 49th Annual Convention of the Computer Society of India CSI Volume 2*. Springer, 2015, pp. 59–70.

[13] M. S. Grewal and A. P. Andrews, *Kalman filtering: Theory and Practice with MATLAB*. Hoboken,NJ: John Wiley & Sons, 2014.

[14] X. R. Li and V. P. Jilkov, "Survey of maneuvering target tracking. part i. dynamic models," *IEEE Transactions on aerospace and electronic systems*, vol. 39, no. 4, pp. 1333–1364, 2003.

[15] Y. Bar-Shalom, X. R. Li, and T. Kirubarajan, *Estimation with applications to tracking and navigation: theory algorithms and software*. John Wiley & Sons, 2001.

[16] R. G. Brown and P. Y. Hwang, "Introduction to random signals and applied kalman filtering: with matlab exercises and solutions," *Introduction to random signals and applied Kalman filtering: with MATLAB exercises and solutions*, 1997.

[17] S. Zhao, Y. S. Shmaliy, S. H. Khan, and G. Ji, "Iterative form for optimal fir filtering of time-variant systems," *RECENT ADVANCES on ELECTROSCIENCE and COMPUTERS*, p. 114, 2015.

[18] S. Zhao, Y. S. Shmaliy, and C. K. Ahn, "Bias-constrained optimal fusion filtering for decentralized wsn with correlated noise sources," *IEEE Transactions on Signal and Information Processing over Networks*, vol. 4, no. 4, pp. 727–735, 2018.

[19] Y. S. Shmaliy, S. Zhao, and C. K. Ahn, "Unbiased finite impluse response filtering: An iterative alternative to kalman filtering ignoring noise and initial conditions," *IEEE Control Systems Magazine*, vol. 37, no. 5, pp. 70–89, 2017.

[20] Y. S. Shmaliy and S. Zhao, *Optimal and robust state stimation:Finite Impulse Response (FIR) and Kalman approaches*. MJohn Wiley Sons, 2022.

[21] R. Padilla, W. L. Passos, T. L. Dias, S. L. Netto, and E. A. da Silva, "A comparative analysis of object detection metrics with a companion open-source toolkit," *Electronics*, vol. 10, no. 3, p. 279, 2021.

[22] F. Sun, H. Li, Z. Liu, X. Li, and Z. Wu, "Arbitrary-angle bounding box based location for object detection in remote sensing image," *European Journal of Remote Sensing*, vol. 54, no. 1, pp. 102–116, 2021.

[23] D. L. Olson and D. Delen, *Advanced data mining techniques*. Springer Science & Business Media, 2008.

[24] (2015) Datasets-visual tracker benchmark. [Online]. Available: http://www.visual-tracking.net

## Contribution of individual authors to the creation of a scientific article (ghostwriting policy)

Eli G. Pale-Ramon has written, reviewed, edited the paper, and implemented the Algorithms in Matlab.
Yuriy S. Shmaliy has developed the methodology; creation of models, and the project administration.
Luis J. Morales-Mendoza and Mario González-Lee has supervised and reviewed the paper, was responsible for the validation metrics, simulation and statistics used.
Silverio Pérez-Caceres and Efrén Morales-Mendoza were responsible for the validation and correction of the computational methods applied, simulation and statistics.

## Creative Commons Attribution License 4.0 (Attribution 4.0 International, CC BY 4.0)